A MULTI-SCALE OBJECT-ORIENTED APPROACH TO THE CLASSIFICATION OF MULTI-SENSOR IMAGERY FOR MAPPING LAND COVER IN THE TOP END.

Tim Whiteside[1,2]

Author affiliation:

[1]Natural and Cultural Resource Management, School of Health and Sciences, Batchelor Institute of Indigenous Tertiary Education, Batchelor, NT 0845.

ph: 08 89397307, fax: 08 89397123, email: tim.whiteside@batchelor.edu.au

[2]Tropical Spatial Science Group, Faculty of Education, Health and Sciences, Charles Darwin University, Darwin, NT 0909.

Abstract

The emergence of robust object-orient methods for the classification of satellite imagery offers viable alternatives to the 'traditional' pixel-based methods. This is particularly of importance when utilising high resolution imagery. This paper describes a multi-scale object-oriented approach to the classification of multi-sensor imagery for mapping land cover in the tropical region of the Northern Territory. After pre-processing, image data was segmented into objects at multiple scale levels. These objects were then assigned class rules using spectral signatures, shape and the contextual relationships of the objects. These rules were used as a basis for the fuzzy classification of the imagery. This method provided results with good accuracy; indicating object-oriented analysis has great potential for extracting land cover information from satellite imagery captured over tropical Australia.

Introduction

Although the concept of image segmentation and object classification is not new (Kettig and Landgrebe 1976), the emergence of robust object-oriented approaches to the classification of remotely sensed data is one of the major advances in digital image processing in recent years (Benz *et al.* 2004). These methods are finding increasing popularity particularly when applied to high resolution satellite imagery (Lennartz and Congalton 2004). The range of resolutions of satellite imagery lends itself to mapping of land cover at a number of scales. High resolution images obviously contain more information than low resolution. Therefore it is reasonable to suggest that coarser resolution data can be used to create small scale land cover maps while higher resolution data can map land cover in greater detail (Colombo *et al.* 2004). Pixels within a low resolution image contain combined signal from a number of objects, where

as pixels within a high resolution image will more closely approximate these objects (Hay *et al.* 2003).

This paper describes a preliminary investigation into the application of an object-oriented method of creating a multi-scale land cover classification from multi-sensor satellite imagery.

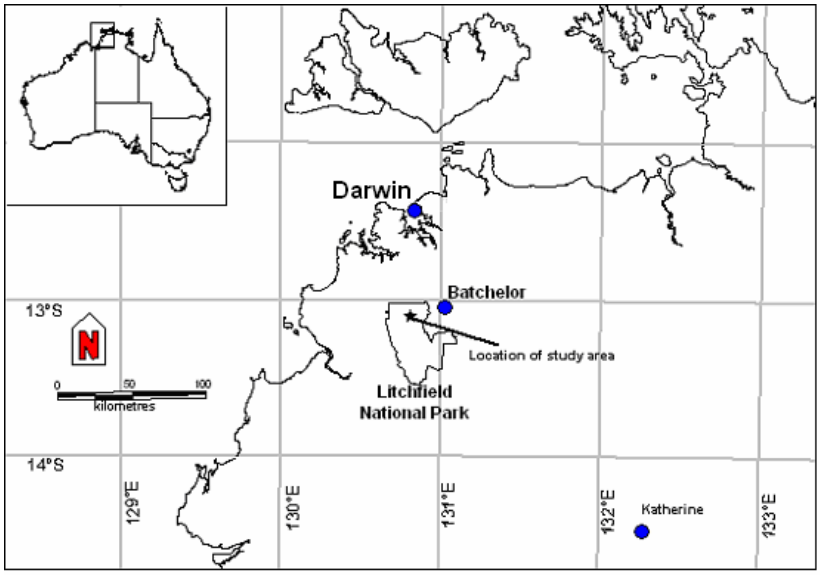

Figure 1: Location of the study area.

Methods

The study area (1373 ha) is located in the Florence Creek region of Litchfield National Park, in the monsoonal north of the Northern Territory of Australia and is approximately 120 km south of Darwin (figure 1). The region's climate is typified by a long dry season (May – September), with little to no rainfall, and an intense wet season. Over 75% of the nearly 1500 mm of annual rainfall falls between November and March. Maximum daily temperatures vary from around 32°C in June and July to over 36°C in October and November.

The southern section of the study area consists of plateau surfaces intersected by drainage lines. Low lying areas subject to inundation are located to the north. Vegetation within the region is predominantly open forest and savanna woodland consisting of a *Eucalyptus* spp. (mostly *E. tetradonta* and *E. miniata*) dominated canopy and annual grass (*Sorghum* spp.) understorey (Griffiths *et al.* 1997). Also found are patches of monsoon closed forest located on springs, near the base of the escarpment and other areas of permanent water. *Melaleuca* spp. forests occur along creek lines and seasonally inundated areas and share overlapping species with the monsoon closed forest (i.e. *Xanthostemon eucalyptoides and Lophostemon lactifluus*) (Lynch and Manning 1988).

Data from two different sensors was used in this project: the Landsat 7 Enhanced Thematic Mapper+ (ETM+) and the Advanced Spaceborne Thermal

Emission and Reflection Radiometer (ASTER). The Landsat 7 ETM+ scene was captured on 29 August 2000 while the ASTER granule was captured on 28 July 2000 and processed to level 1B (Abrams 2000). ASTER products provide 14 spectral bands, 3 in the visible and near infrared (0.52-0.86 µm), 6 in the shortwave infrared (1.60-2.43 µm) and 5 in the thermal infrared bands (8.12-11.65 µm) (Yamaguchi *et al.* 1998). The near infrared band 3 is captured at nadir (3N) and backwards looking (3B), creating an along-track stereo pair of images (Abrams 2000). The relative DEM based on ASTER bands 3N and 3B from the above granule was requested and acquired in October 2002.

The Landsat ETM+ image was registered to the ASTER image using ERDAS Imagine image processing software and subsets for the study area were created from the images and DEM (figure 2).

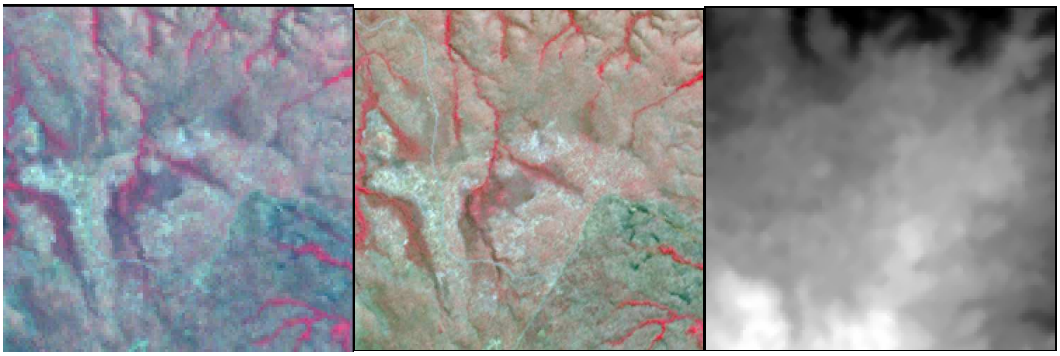

(a) (b) (c)

Figure 2: The subsets of (a) the Landsat 7 ETM+ (4, 3, 2 = RGB), (b) the ASTER data (3N, 2, 1 =RGB) and (c) corresponding DEM subset. covering the study area.

The subset images were segmented into objects using eCognition v4 software (Baatz *et al.* 2004). Segmentation occurred on two scale levels (figure 3). The segmentation of the images into objects was influenced by three parameters: scale, colour and form (Willhauck *et al.* 2000). The scale parameter set by the operator is influenced by the heterogeneity of the pixels. The colour parameter is a balance between the homogeneity of a segment's colour and the homogeneity of its shape. The form parameter balances the smoothness of an object's border with its compactness. The homogeneity criterion for the objects is established in the weighting of these parameters. A visual inspection of the objects resulting from variations parameter weighting was used to determine the overall values for the weighting of the parameters at each scale level (table 1).

Table 1: Segmentation parameters.

Scale level	Data	Scale parameter	Shape factor	Compactness	Smoothness
2	Landsat 7 ETM+	15	0.3	0.7	0.3
1	ASTER	5	0.2	0.7	0.3

At scale level 2, a total of five land cover classes were identified for the study area. These classes were based upon the characteristic vegetation and knowledge of the area. At scale level 1, a total of ten land cover classes were identified based on the structural formation of the vegetation and characteristic Genus. Two of these classes were introduced to include areas of the study site that were identified as recently burnt. Class rules for the objects were then developed using spectral signatures, shape, location and the contextual relationships of the objects. These rules were then used as a basis for classification of the image and DEM. Selected image objects were then used as samples for each class to act as training areas for the classification process.

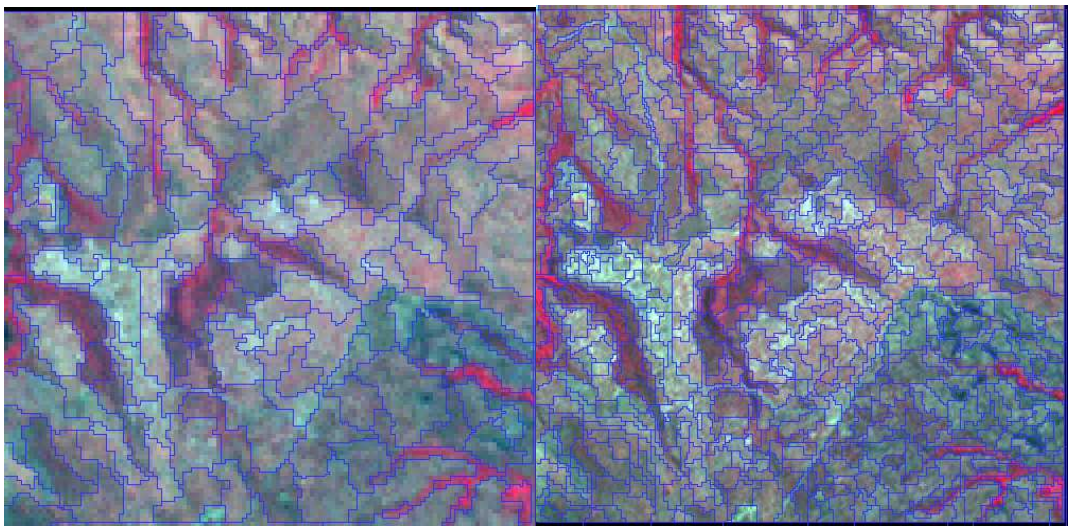

(a) (b)

Figure 3: The study area showing the hierarchical segmentation at (a) level 2 draped over the Landsat 7 ETM+ subset and (b) level 1 draped over the ASTER subset.

The image was classified using eCognition software's method of fuzzy logic (Baatz*, et al.* 2004). Once classified, image objects have membership of varying degrees or probability to several classes. The class with the highest probability value is then assigned as the best or most suitable class for each object (Benz*, et al.* 2004). Accuracy of the fuzzy classification was determined based on the mean probability of the best classification and the mean stability of each class (Baatz*, et al.* 2004). The mean stability is the difference between the probability of an object belonging to the best class and the probability of an object belonging to the next class - the higher the value the greater the stability.

Results

The classification of the level two segmentation can be seen in figure 4. Five broad land cover classes are displayed. A summary of the accuracy assessment of the level 2 fuzzy classification is presented in table 2. The Mean

p_{1st} column displays the mean probability of objects belonging to that class. All classes have a mean p_{1st} value over 0.8 suggesting that the probability of image objects being assigned the best class was high. The class with the lowest value is Grassland suggesting that objects assigned this class have only have a probability of 0.81 of being classed correctly. Within the Mean stability column most of the classes display low stability in their classification. The Eucalypt open forest, Grassland and Mixed woodland classes have a Mean stability value under 0.1, suggesting that a number of objects within these classes may not have been assigned to the correct class.

Figure 4: Level 2 classification

Table 2: Accuracy of the level 2 classification.

Class	Class name	Mean p_{1st}	Mean stability
1	Eucalypt woodland	0.827	0.105
2	Eucalypt open forest	0.859	0.078
3	Grassland	0.810	0.078
4	Mixed woodland	0.850	0.037
5	Riparian	0.885	0.221

The image resulting from the level 1 object-oriented classification is shown in figure 5. The number of objects classified and the area (ha) assigned each class are presented in table 3. According to the classification the land cover class occupying the largest area is Eucalypt woodland (376 ha) with the number of objects identified as belonging in that class being 675. The land cover with the smallest area within the study site is Grassland occupying only 15 ha and consisting of just 21 image objects.

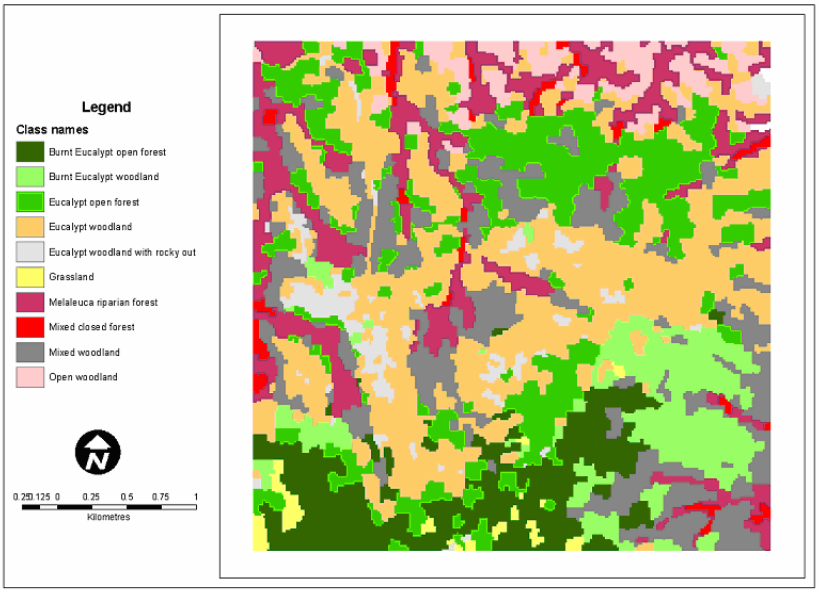

Figure 5: Level 1 classified image.

Table 3: Areas (ha) classified for level 1 classification.

Class ID	Class code	Class name	No. objects	Area (ha)
	1	Burnt Eucalypt open forest	128	228.38
	2	Eucalypt open forest	205	140.54
	3	Mixed closed forest	35	19.58
	4	*Melaleuca* riparian forest	215	168.09
	5	Eucalypt woodland	675	376.02
	6	Burnt Eucalypt woodland	118	114.39
	7	Eucalypt woodland with rocky outcrops	83	42.59
	8	Open woodland	71	57.55
	9	Mixed woodland	214	208.84
	10	Grassland	21	15.18

Table 4 is a summary of the accuracy assessment of the level 1 fuzzy classification. Nearly all classes have a mean p_{1st} value over 0.8 suggesting that the probability of image objects being assigned the best class was high. The Open woodland class has the lowest value suggesting that objects assigned this class have only have a probability of 0.68 of being classed correctly. Within the Mean stability column most of the classes display stability in their classification. Only the Eucalypt open forest, *Melaleuca* riparian forest and Mixed woodland classes have a Mean stability value under 0.1 meaning that a number of objects within these classes may not have been assigned to the correct class.

Table 4: Fuzzy classification accuracy assessment for level one classification.

Class	Class name	Mean p_{1st}	Mean stability
1	Burnt Eucalypt open forest	0.880	0.136
2	Eucalypt open forest	0.827	0.092
3	Mixed closed forest	0.810	0.362
4	*Melaleuca* riparian forest	0.796	0.048
5	Eucalypt woodland	0.832	0.145
6	Burnt Eucalypt woodland	0.856	0.373
7	Eucalypt woodland with rocky outcrops	0.839	0.362
8	Open woodland	0.676	0.373
9	Mixed woodland	0.874	0.048
10	Grassland	0.840	0.138

Discussion

The work presented shows a method of producing land cover classification at multiple scales using an object oriented approach. While this work is in its initial stages, the results show that this approach has potential for mapping land cover in tropical Australia. The accuracy of the majority of classes was good with only a couple of classes showing poor stability. Further work is needed to refine the scale parameters used within the segmentation process. Other research to be undertaken includes increasing the knowledge base of the classes prior to classification using further topological relationships and including the use of ancillary data such as derivative data sets or slope layers. Another aim is to extend range of the project to incorporate the use of high resolution imagery such as Quickbird to undertake a further level of segmentation and to conduct a classification of a much larger area.

References

ABRAMS, M., 2000, The Advanced Spaceborne Thermal Emission and Reflection Radiometer (ASTER): data products for the high spatial resolution imager on NASA's Terra platform. *International Journal of Remote Sensing*, **21**, 847-859.

BAATZ, M., BENZ, U., DEHGHANI, S., HEYNEN, M., HÖLTJE, A., HOFMANN, P., LINGENFELDER, I., MIMLER, M., SOHLBACH, M., WEBER, M., & WILLHAUCK, G., 2004, *eCognition Professional: User guide 4.* (Munich: Definiens-Imaging).

BENZ, U., HOFMANN, P., WILLHAUCK, G., LINGENFELDER, I., & HEYNEN, M., 2004, Multi-resolution, object-oriented fuzzy analysis of remote sensing data for GIS-ready information. *ISPRS Journal of Photogrammetry and Remote Sensing*, **58**, 239-258.

COLOMBO, S., CHICA-OLMO, M., ABARCA, F., & EVA, H., 2004, Variographic analysis of tropical forest cover from multi-scale remotely

sensed imagery. *ISPRS Journal of Photogrammetry and Remote Sensing*, **58**, 330-341.

GRIFFITHS, A. D., WOINARSKI, J. C. Z., ARMSTRONG, M. D., COWIE, I. D., DUNLOP, C. R., & HORNER, P. G., 1997, *Biological Survey of Litchfield National Park.* Report no. 62, PWCNT, Darwin.

HAY, G. J., BLASCHKE, T., MARCEAU, D. J., & BOUCHARD, A., 2003, A comparison of three image-object methods for the multi-scale analysis of landscape structure. *ISPRS Journal of Photogrammetry and Remote Sensing*, **57**, 327-345.

KETTIG, R. L., & LANDGREBE, D. A., 1976, Classification of multispectral image data by extraction and classification of homogeneous objects. *IEEE Transactions on Geoscience Electronics*, **GE-14**, 19-26.

LENNARTZ, S. P., & CONGALTON, R. G., 2004, Classifying and mapping forest cover types using IKONOS imagery in the norteastern United States in *ASPRS Annual Conference Proceedings,* 23-28 May, (Denver, Colorado).

LYNCH, B. T., & MANNING, K. M., 1988, *Land resources of Litchfield Park*. Report no. 36, Conservation Commission of the Northern Territory, Darwin.

WILLHAUCK, G., SCHNEIDER, T., DE KOK, R., & AMMER, U., 2000, Comparison of object-oriented classification techniques and standard image analysis for the use of change detection betweeen SPOT multispectral satellite images and aerial photos in *XIX ISPRS Congress,* 16-22 July, (Amsterdam).

YAMAGUCHI, Y., KAHLE, A. B., TSU, H., KAWAKAMI, T., & PNIEL, M., 1998, Overview of Advanced Spaceborne Thermal Emission and Reflection Radiometer (ASTER). *IEEE Transactions on Geoscience and Remote Sensing*, **36**, 1062-1071.